Available online at www.sciencedirect.com
SCIENCE DIRECT®
International Journal of Heat and Fluid Flow 24 (2003) 199–209
International Journal of HEAT AND FLUID FLOW
www.elsevier.com/locate/ijhff

Effects of acoustic excitation positions on heat transfer and flow in axisymmetric impinging jet: main jet excitation and shear layer excitation

S.D. Hwang, H.H. Cho *

Department of Mechanical Engineering, Yonsei University, 134, Shinchon-dong, Seodaemun-gu, Seoul 120-749, South Korea

Received 13 November 2001; accepted 2 October 2002

Abstract

An experimental study is conducted to investigate the flow and heat transfer characteristics of an impinging jet with acoustic excitations. Two different acoustic excitation methods based on the locations of the actuator are tested and compared: one is a main jet excitation and the other is a shear layer excitation. Effects of excitation level on the heat transfer and flow characteristics are also investigated. Local Nusselt number distributions are measured on the impingement surface and velocity and turbulence intensity distributions are also measured. The forcing Strouhal numbers (excitation frequency, *St*) are 1.2, 2.4, 3.0 and 4.0 and the excitation level varies from 80 to 100 dB. When the vortex pairing is promoted by the excitation *St* of 1.2 with the main jet excitation, low heat transfer rates are obtained at the large nozzle-to-plate distances. For the excitation *St* of 2.4 with the main jet excitation, high heat transfer rates are obtained at the large gap distances due to the extended potential core length. The main jet excitation method shows similar heat and flow characteristics to the shear layer excitation although the basic flow schemes and the location of the forcing actuator are different. The effects of the acoustic excitation to the jet increase as the excitation level increases. Therefore, the excitation frequency and the excitation level are both important factors in the acoustic excitation.

Keywords: Vortex pairing; Main jet excitation; Shear layer excitation; Heat transfer coefficients; Impingement jet; Excitation frequency; Excitation level

1. Introduction

Heat transfer under an impinging jet is generally superior to that achieved with a typical convective heat transfer method. With an impinging jet, it is easy to adjust the location of interest and to remove a large amount of heat on the impingement surface. For these reasons, the impinging jet cooling/heating technique has been widely used in many industrial systems such as cooling of high temperature gas turbines, drying of paper or textiles, and processing of steel or glass. In recent years, it has been applied to cool high-density electrical and electronic equipment. Therefore, heat transfer and fluid flow characteristics between a single jet or multiple impinging jets and a flat surface have been the subjects of numerous investigations for many years. However, the details of the flow structures and heat transfer mechanism have not been stated clearly.

Gardon and Akfirat (1965) and Hoogendoorn (1977) examined the local heat transfer coefficient on the impinging surface influenced by the turbulence. Martin (1977) summarized the heat and mass transfer characteristics of impinging jets for the different nozzle types and configurations: single round nozzle, single slot nozzle, arrays of round nozzle and arrays of slot nozzle. Huang and El-Genk (1994) conducted experimental study to determine the values of the local and average Nusselt numbers for the heat transfer between a uniformly heated flat plate and an impinging circular air jet, particularly for the small values of Reynolds number and jet spacing. Jambunathan et al. (1992) and Viskanta (1993) reviewed extensively numerous studies of jet impingement heat transfer.

* Corresponding author. Tel.: +82-2-2123-2828; fax: +82-2-312-2159.
E-mail address: hhcho@yonsei.ac.kr (H.H. Cho).

0142-727X/03/$ - see front matter © 2002 Elsevier Science Inc. All rights reserved.
doi:10.1016/S0142-727X(02)00236-9

Nomenclature

A	impingement surface area (m^2)
D	nozzle exit diameter (= 24.6 mm)
f	acoustic excitation frequency (Hz)
H	nozzle-to-plate distance
h	convective heat transfer coefficient (W/m^2 K)
I	electric current (A)
k	thermal conductivity of the air (W/mK)
Nu	local Nusselt number (hD/k)
Nu_0	Nusselt number at the stagnation point
$Nu_{0,2D}$	Nusselt number of the non-excited jet at the stagnation point of $H/D = 2$
$Nu_{0,12D}$	Nusselt number of the non-excited jet at the stagnation point of $H/D = 12$
$Nu_{0,St=0}$	Nusselt number of the non-excited jet at the stagnation point
q_w	surface heat flux (W/m^2)
q_c	conduction loss (W/m^2)
R	electric resistance of the heating foil (Ω)
r	radial direction coordinate
Re	Reynolds number (UD/v)
St	Strouhal number (fD/U)
T_{aw}	jet adiabatic wall temperature
T_j^0	total temperature of jet flow
T_w	wall temperature
U	average nozzle exit velocity of the jet
$\bar{u}$	mean streamwise velocity
u'	fluctuating velocity ($\sqrt{u'^s}$)
x	streamwise coordinate
v	dynamic viscosity

Subscripts

s	shear layer excitation
m	main jet excitation
exit	center of nozzle exit
o	stagnation point

The flow characteristics of impinging jet are affected by an ejected jet flow condition. The reason is that the vortices at free shear layer are generated by the initial Kelvin–Helmholts instabilities and the vortex ring grows, and vortex pairing process occurs as the jet flow develops. Therefore, the flow and heat transfer characteristics on the impingement surface can be changed by the controlling of the vortices.

Several techniques are applied to control the vortices such as additional secondary flows to the jet periphery, changes of nozzle exit shapes and conditions and an acoustic excitation. The acoustic excitation method is forcing the sound waves to the jet flows, resulting that the flow and heat transfer characteristics are affected by the forcing frequencies. Thus, the heat transfer rates can be enhanced or reduced on the impingement surface by the forcing the flows with the proper excitation frequency.

Cho et al. (1998) and Lee et al. (1998) investigated the heat transfer characteristics with the additional secondary flows to the jet periphery for the different nozzle types, such as a circular contoured nozzle and a circular pipe nozzle. Crow and Champagne (1971) forced the flow with the specific frequency and amplitude, and they found that the jitters generated at the shear layer reduced when the flow is excited with the frequency of $St = 0.3$, and called it a preferred mode. Zaman and Hussain (1980a,b) found that the turbulence intensity of the flow is lower than that of the non-excited jet with the excitation St of 1.6 and 2.4. Gau et al. (1997) showed that flow structure was significantly altered by the acoustic excitation with inherent or non-inherent frequency. At the inherent frequency, that is a half or a quarter of the fundamental frequency, the turbulence intensity increased and heat transfer enhanced with the acoustic excitation. Liu and Sullivan (1996) showed that enhancement and reduction of the local heat transfer in the wall jet region can be attained by forcing the impinging jet near the natural frequency and its subharmonic respectively. In our previous study (Hwang et al., 2001), the flow and heat transfer characteristics of the impinging jet are investigated by the control of the vortex pairing; secondary flows and acoustic excitations and compared the results. For the acoustic excitation, the vortex frequencies of the jet flows are not directly related to the excitation frequency itself. The subharmonic frequency of the excitation frequency has an important role to the control of vortex generation and pairing process.

This study focuses on the effects of the acoustic excitation methods based on the location of the actuator (main jet excitation and shear layer excitation). The results obtained from the main jet excitation are compared with those of the shear layer excitation. The main jet excitation method is forcing the jet flows before ejection from the nozzle exit and the shear layer excitation is forcing the jet flows with the acoustic waves to the jet periphery at the nozzle exit. The effects of excitation level (sound pressure level of the excitation frequency; dB) are also investigated. The mean velocity and turbulence intensity distributions are measured using a hot-wire anemometer. The local Nusselt numbers on the impingement surface are measured for the nozzle-to-plate spacing (H/D) from 2 to 16. The forcing Strouhal numbers (excitation frequency, St) are 1.2, 2.4, 3.0 and 4.0 with the excitation level of 95 dB and the

excitation levels are changed from 80 to 100 dB for investigating the effects of the excitation level. The nozzle exit Reynolds number of the main jet is fixed at 34,000 for all tested cases.

2. Experimental setup and procedure

Fig. 1(a) shows the experimental apparatus of the acoustic excitation systems. The acoustic waves are created by a generating program (CoolEdit96) and sound card (SB32) in the PC. The sound signal is amplified by an amplifier and supplied to the woofer speaker (200 W). Sound waves generated by the woofer are supplied to a shear layer excitation device or a main jet excitation device. The acoustic waves and signals are verified by the microphone and oscilloscope, and the sound pressure level of the excitation frequency at the nozzle exit is also confirmed by the sound pressure level meter (dB meter, TES1350) with the resolution of 0.1 dB. The location of the forcing actuator is shown in Fig. 1(a). For the shear layer excitation (Fig. 1(a)—part A), the excitation device is installed at the nozzle exit and the sound waves are supplied from the woofer speaker through the flexible tube of 9 mm in diameter. For the main jet excitation (Fig. 1(a)—part B), the acoustic waves is fed by the circular chamber and excites the main flows directly. The sound-absorbing material sheets are installed on the laboratory walls and surrounding of the experimental setup to reduce the background noises.

The main flow is supplied from a blower (3.7 kW) and passes through a heat exchanger which maintains a uniform jet temperature within ±0.2 °C of the ambient temperature and a silencer. The role of the silencer is to reduce the flow fluctuations and the sound waves that are generated at the blower. The flow rates are measured using a thin plate orifice flowmeter within ±0.1% accuracy. A smoothly contoured nozzle is designed to obtain a uniform velocity profile (top hat) with a large contraction ration of 50:1 (Morel, 1977). The nozzle exit diameter (D) is 24.6 mm.

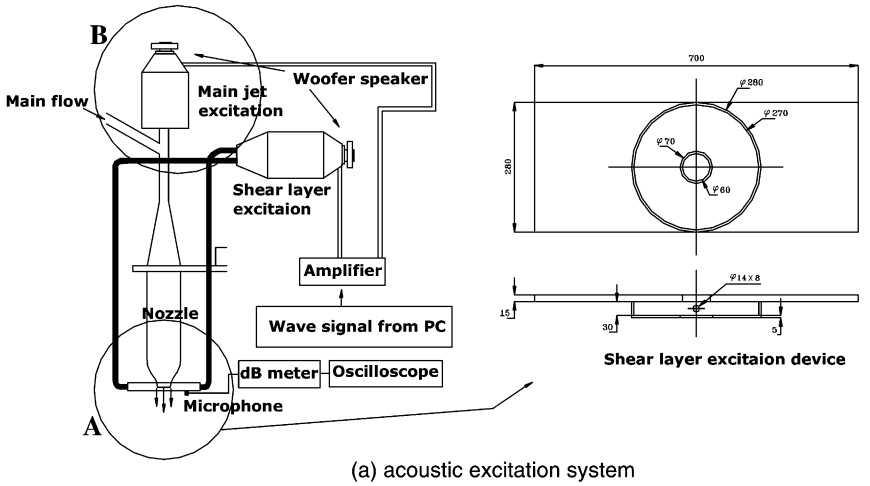

(a) acoustic excitation system

(A : the shear layer excitation device B : the main jet excitation device)

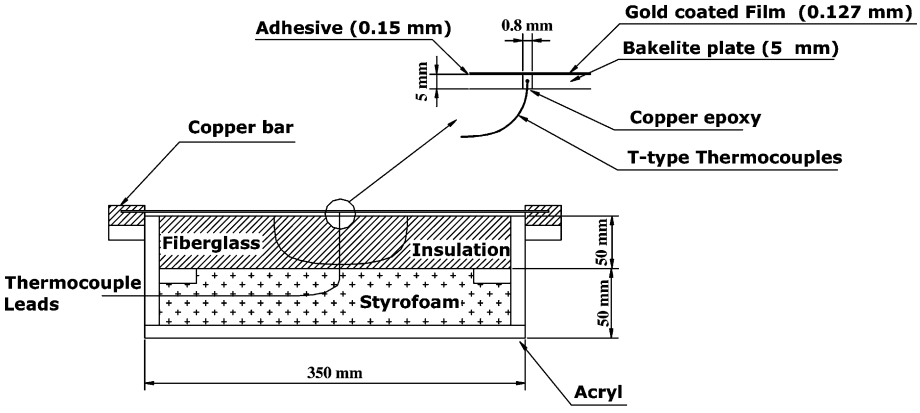

(b) impingement plate

Fig. 1. Schematic diagram of experimental apparatus.

Mean velocity and turbulence intensity are measured by a hot-wire anemometer (TSI-IFA300) which is a constant temperature type with the I-probe sensor. A three-axis traverse controlled by the PC is used to move the hot-wire probe in the axial and radial directions. The measured data are stored in the PC through GPIB board. The sampling rate is 4000 Hz and the number of sampled data is 4096 points, and a low pass filter (LPF) of 2000 Hz is used for all these procedures.

Local surface temperature or heat transfer coefficients on the impingement surface are measured by the thermocouples under a constant heat flux condition. Fig. 1(b) shows the cross-section of the impingement test plate. The test plate includes a thin gold-coated film (Aure-12) of 125 μm in thickness bonded on a thin laminate plate of 5 mm in thickness using a double-sided adhesive tape. The laminate plate is insulated with a 50 mm Styrofoam and a 50 mm thick fiberglass. In order to obtain a constant heat flux condition, two large copper bus bars, placed at each end of the gold-coated film, are connected to the power supply through a voltage trap (shunt) to measure the current. Thirty-five thermocouples (36-gauge, T-type) are embedded in the laminate plate beneath the gold-coated film with a spacing of 0.2 D in the radial direction. Thermal epoxy (copper oxide) is used as a filling cement and an electrical insulator for the gold-coated film. The temperature measuring system consists of a switching system (Keithley model 7001), a multimeter (Keithley model 2001) and a personal computer.

The convective heat transfer coefficient is defined by

$$h = \frac{q_w}{T_w - T_{aw}} \tag{1}$$

where q_w is the heat flux from the surface, T_w is the wall temperature, and T_{aw} is the jet adiabatic wall temperature. Since the flow velocity of the jet is low, the adiabatic wall temperature (T_{aw}) is nearly equally to the jet total temperature (T_j^0) (Hwang et al., 2001). Therefore, the local heat transfer coefficient can be written by

$$h = \frac{q_w}{T_w - T_j^0} \tag{2}$$

and q_w is obtained as

$$q_w = I^2 \frac{\overline{R}}{A} - q_c \tag{3}$$

where I is the electric current in the gold-coated film, $\overline{R}$ is the overall electric resistance of the heating foil, and A is the area of the impingement surface. q_c is conduction loss through insulation material. The radiation heat loss is neglected since the present experiment is conducted with the surface temperature below 50 °C. The electric current is controlled by a variable power supply and measured precisely using a shunt within ±1.0% accuracy.

Experimental results for heat transfer are presented in terms of the Nusselt number

$$Nu = \frac{hD}{k} = \frac{q_w}{T_w T_j^0} \frac{D}{k} \tag{4}$$

where k is the conductivity of the jet air. Using a methodology outlined by Kline and McClintock (1953), the uncertainty in the 95% confidence level is about 3% in the Nusselt number. The uncertainty is attributed mainly to the uncertainty of the calculation of the surface heat flux, q_w.

3. Results and discussion

3.1. Main jet excitation

3.1.1. Flow characteristics

The Strouhal number, St, indicates the frequency characteristics of the flow and is defined by

$$St = \frac{fD}{U} \tag{5}$$

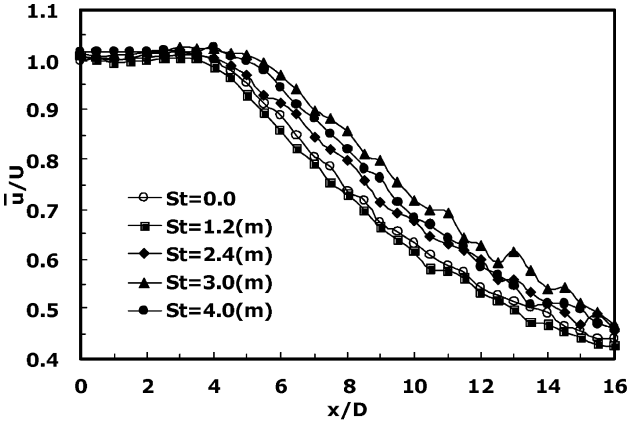

(a) mean streamwise velocity

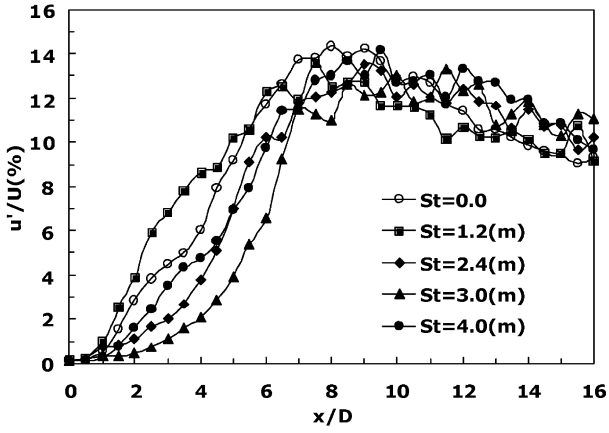

(b) turbulence intensity

Fig. 2. Effect of St on mean streamwise velocity and turbulence intensity along the centerline of free jet with the main jet excitation (Re = 34,000).

where f is the forcing frequency of the acoustic excitation or generating vortex frequency. In this study, St is the forcing frequency of acoustic excitation and $St = 0$ means the conventional jet without acoustic excitation.

Fig. 2 shows the variation of the mean streamwise velocity and turbulence intensity distributions measured along the centerline of the jet. Legend "(m)" indicates the results using the main jet excitation. For the free jet without the acoustic excitation, a ring vortex is created around the jet periphery by the virtue of the instability of the mixing layer and moves downstream. As the vortex moves downstream, it undergoes a process of pairing and development. When the vortex generated at the mixing layer grows in size, it affects the core of the jet flow and finally the potential core disappears. In the case of non-excited jet ($St = 0.0$), the flow maintains uniform nozzle exit velocity for a distance of $4D \sim 5D$ (potential core). As the flow is developing and the vortices are growing, the velocity of the jet decreases monotonically. The turbulence intensity is low at the nozzle exit and increases steadily until $x/D \cong 8$. When the jet flow is fully developed, the turbulence intensity decreases slowly. With the acoustic excitation, the general trends of the mean velocity distributions are similar to those of the non-excited jet, but the jet potential core lengths are changed. When the vortex pairing and development of the jet are suppressed by the acoustic excitation frequency of $St = 2.4$ and 3.0, the potential core length is longer than that of the non-excited jet and the turbulence intensity increases slowly, resulting in lower values within the potential core region. In the case of $St = 1.2$, the jet flow has a shorter core length and a higher

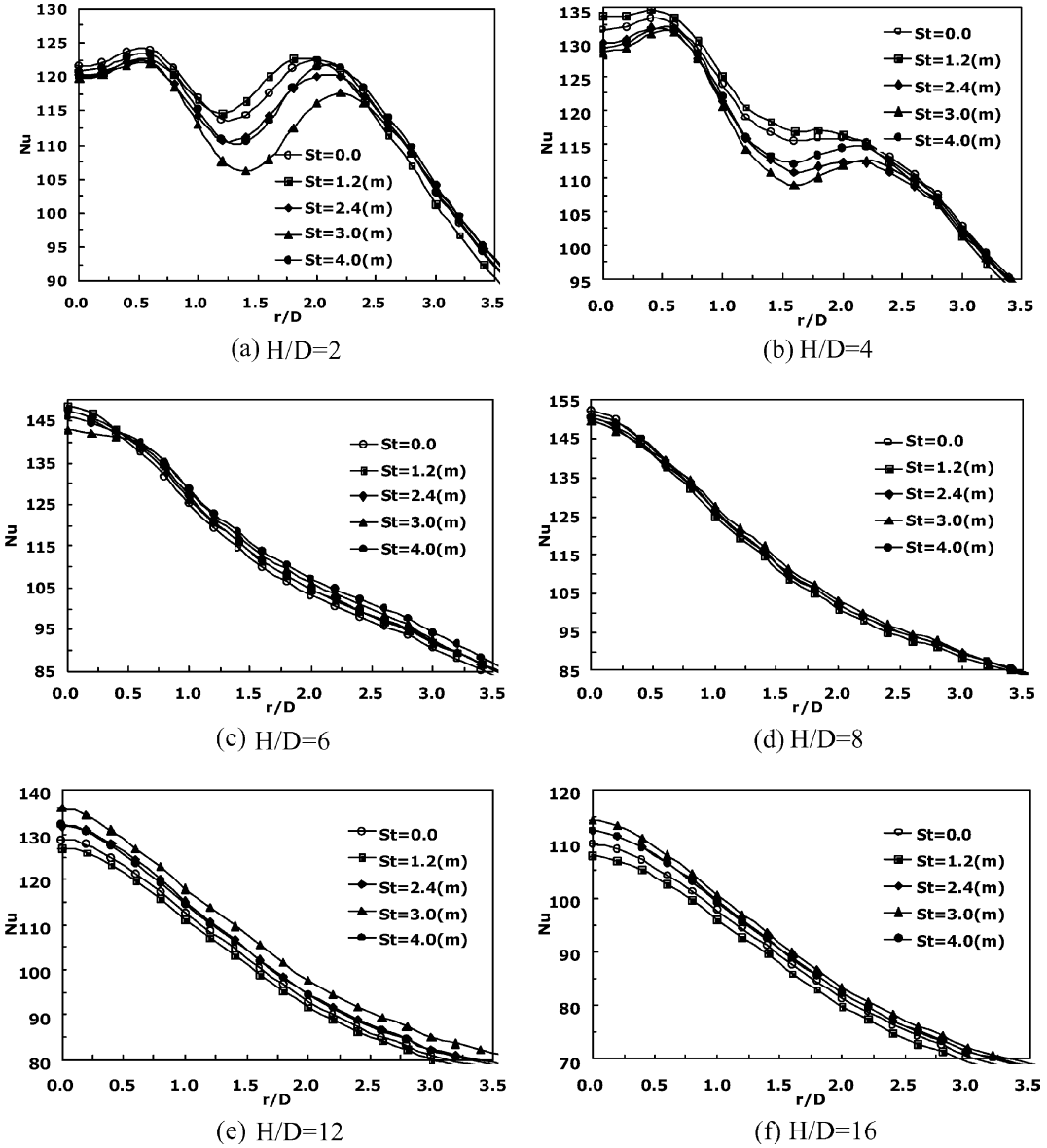

Fig. 3. Effects of H/D and St on radial distribution of Nu with the main jet excitation ($Re = 34{,}000$).

turbulence intensity within the potential core due to the promotion of vortex pairing and the development of the jet core flow. When the jet flows are fully developed, for $x/D \geqslant 10$, turbulence intensities are similar for all tested cases. For the case of $St = 4.0$, similar mean velocity and turbulence intensity values are obtained to the values of the excited $St = 2.4$.

These results are related to the natural frequency characteristics of the free jet. The natural frequency of the jet flow is St of 1.2, which is the fundamental frequency of the initial vortex generation in this study. When the flow is excited with the excitation St of 2.4, the subharmonic frequency of the excitation St of 2.4, that is the fundamental frequency of the jet flow ($St = 1.2$), is reinforced resulting in the suppression of the flow development and vortex pairing process. In case of the excitation frequency of $St = 1.2$, the half frequency component of the excitation St of 1.2, that is $St = 0.6$ which is the frequency of the jet vortex pairing, is reinforced by the acoustic excitation. Hence the vortex pairing and the flow development are promoted resulting in high turbulence intensity and shorter potential core length. More detailed frequency characteristics of the jet flow used in this study are explained in our previous study (Hwang et al., 2001). For the excitation St of 3.0 and 4.0, it shows similar effects to that of the excitation St of 2.4.

3.1.2. Heat transfer characteristics

Fig. 3 shows the effects of H/D and St on the radial distribution of Nusselt numbers. The non-excited jet shows some distinct heat transfer characteristics on the impingement surface. For a small nozzle-to-plate spacing ($H/D = 2$ and 4), there are two local peaks in Nusselt number. The first peak at $r/D \cong 0.5$ is caused by the effect of stagnation flow acceleration. The flow acceleration reduces the boundary layer thickness resulting in the heat transfer increase. The secondary peak appears at $r/D \cong 2$. Generally, it is considered that the secondary peak in the Nusselt number is induced by the flow transition from laminar to turbulence and by the secondary vortices generated at $r/D \cong 2$. The vortices near the wall disturb the boundary layer flow and enhance the mixing of ambient fluids, creating the peak value of the Nusselt number. As the gap distance increases ($H/D \geqslant 8$) and the impingement plate is located outside of the jet potential core, there is only one peak at the stagnation point. This is because the jet flow is fully developed and the turbulence intensity at the stagnation region is sufficiently high, as shown in the flow characteristics of the free jet.

For the excitation frequency (St) of 2.4 and 3.0, the heat transfer rates at the small gap distance of $H/D = 2$ and 4 are lower than those of the non-excited jet for $r/D \leqslant 2.5$ and the position of the secondary peak of the Nusselt number moves outward in the radial direction due to the delay of the flow transition. It is because the excited jet flow has relatively high velocity and low turbulence intensity values for the small gap distances. For the case of $St = 1.2$, the heat transfer rates are slightly higher than those of the non-excited jet for the small gap distance. At the medium gap distance of $H/D = 6$ and 8, the similar distributions of the Nusselt number are obtained for the all excitation frequency. The reason is that the impinging plate is located about the end of potential core region and the flow has relatively high turbulence intensity for the all cases. At the large gap distance ($H/D = 12$ and 16), the high heat transfer rates are obtained with the excited frequency of $St = 2.4$ and 3.0. However, the Nusselt number for $St = 1.2$ is slightly lower than that of the non-excited jet. For the excited St of 4.0, similar Nusselt number distributions to the case of $St = 2.4$ are obtained.

As a result, heat transfer characteristics on the impingement surface are affected by the change of jet flow structures. When the development of jet flows is promoted by the acoustic excitation of $St = 1.2$, heat transfer rates are enhanced a little at the small gap distances due to the high turbulence intensity. However, the heat transfer rates are slightly lower at the large gap distances due to the lower jet stream velocity. Con-

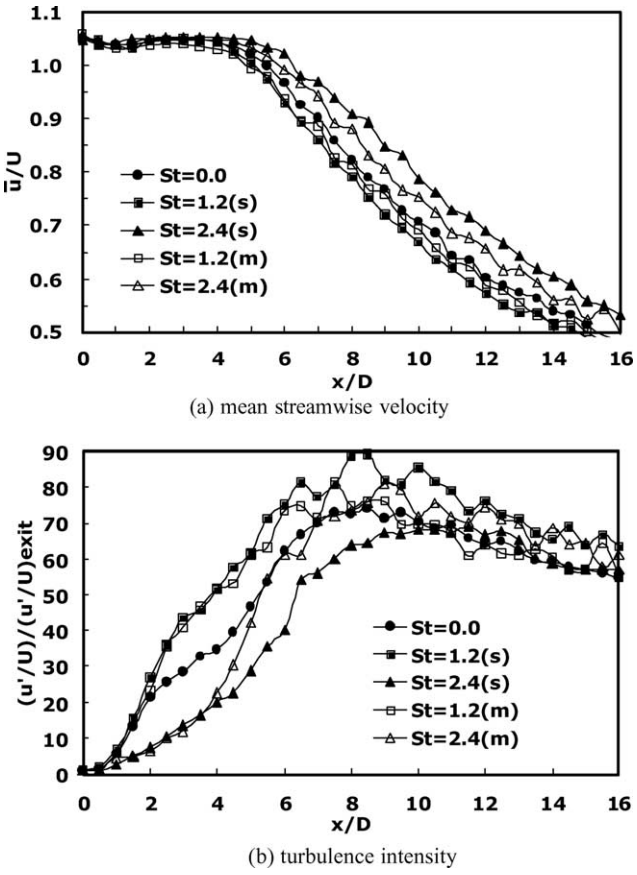

Fig. 4. Comparison of mean streamwise velocity and turbulence intensity between shear and main jet excitation for $St = 1.2$ and 2.4 ($Re = 34{,}000$).

versely, when the flow is excited with the *St* of 2.4 and 3.0, the heat transfer rates are reduced a little at the short gap distances and formation of the secondary peak of heat transfer coefficients is delayed due to the low turbulence intensity of the jet core flow. Enhancements in heat transfer rates are obtained at the large gap distances by the suppression of vortex pairing and development of the jet resulting in extended potential core length with $St = 2.4$ and 3.0.

3.2. Comparison of shear layer excitation and main jet excitation

3.2.1. Flow characteristics

The main jet excitation method is forcing directly the main jet flows and the shear layer excitation method is exciting the jet flow circumferentially at the nozzle exit. This classification is based on the location of the forcing actuator. In this section, the results of the main jet excitation are compared with the results of the shear layer excitation to investigate the effects of the excitation positions. Fig. 4 presents the comparison of the velocity and turbulence intensity distributions along the centerline of the free jet between the main and shear layer jet excitations for $St = 1.2$ and 2.4. The legends "(m)" and "(s)" indicate the results of the main jet excitation and the shear layer excitation respectively. When the vortex pairing processes and developments of the jet are suppressed by both excitation *St* of 2.4(m) and 2.4(s), longer potential core length and lower turbulence intensity are obtained than that of the non-excited jet within the potential core region. However, the main jet excitation method shows a little shorter potential core length and a little higher turbulence intensity than those of the shear layer excitation method. In both cases of $St = 1.2$(m) and $St = 1.2$(s), the jet flow has a shorter potential core length and a higher turbulence intensity in the potential core region due to the promotion of vortex pairing and jet flow development. Both excitation methods show similar effects on the flow characteristics in jet though the position of the actuator is different.

3.2.2. Heat transfer characteristics

The heat transfer characteristics of the impinging jet with the main jet and shear layer excitations are compared in Fig. 5. The symbol, $Nu_{0,St=0}$, indicates the Nusselt number of the non-excited jet at the stagnation point for each nozzle-to-plate spacing. For the small nozzle-to-plate distance ($H/D = 2$ and 4), the Nusselt numbers with the excitation *St* of 2.4 for both excitation methods are lower than those of the non-excited jet. The position of the secondary peak of the Nusselt number

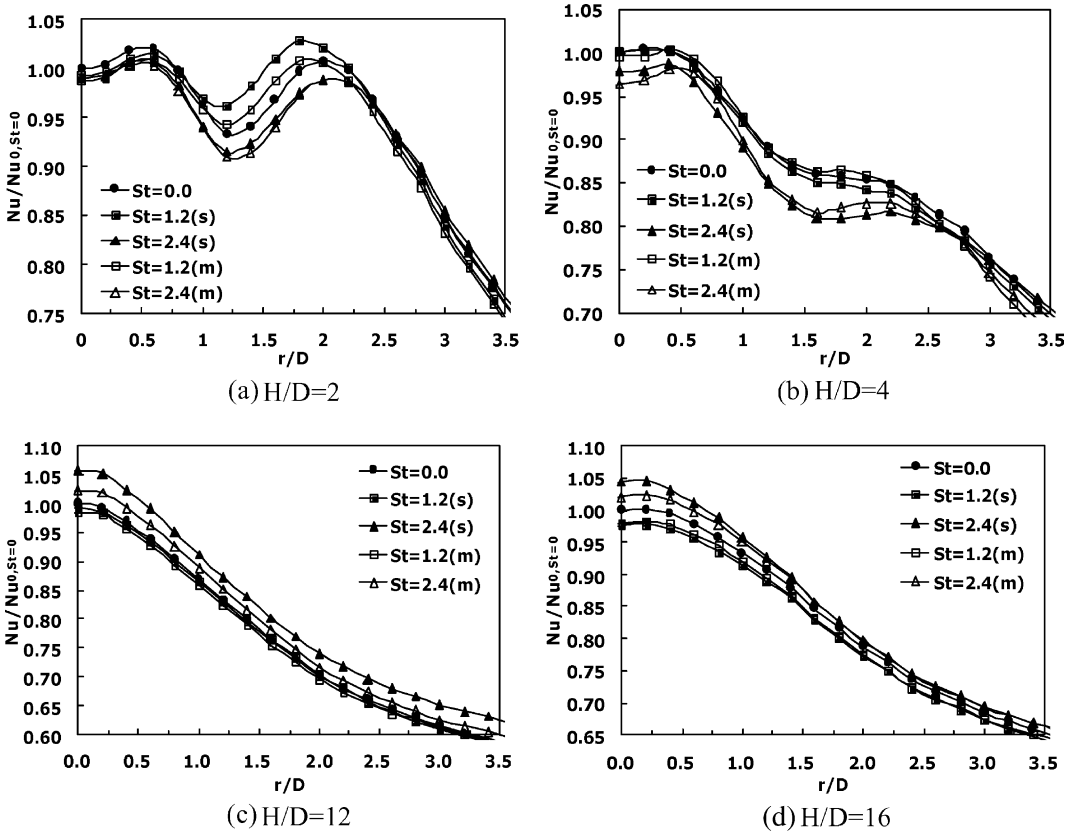

Fig. 5. Comparison of *Nu* between shear and main jet excitation for $St = 1.2$ and 2.4 ($Re = 34{,}000$).

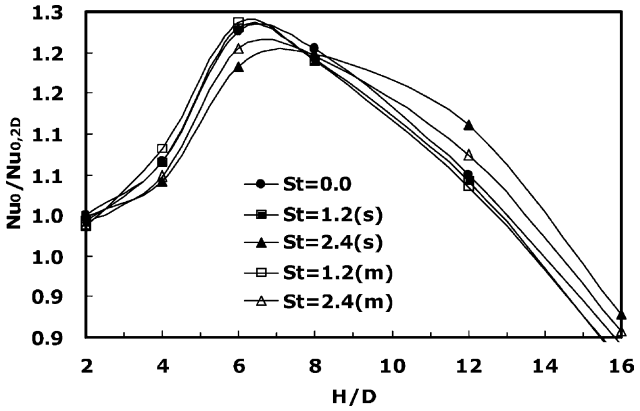

Fig. 6. Effect of St on variation of Nu at stagnation point with H/D for $St = 1.2$ and 2.4 ($Re = 34{,}000$).

moves outward in the radial direction with the excitations. At the large gap distances ($H/D \geqslant 12$), the high heat transfer rates are obtained with the excited frequency of $St = 2.4$(m) and $St = 2.4$(s). However, heat transfer rates for $St = 1.2$(m) and $St = 1.2$(s) are slightly lower than those of the non-excited jet.

Fig. 6 presents the normalized Nusselt number at the stagnation point for various H/D. The maximum Nusselt number at the stagnation point appears at $H/D = 6$–8 and it is because the flow has relatively high velocity and turbulence intensity within the potential core region. After $H/D = 8$, the heat transfer rates at the stagnation point decrease due to the decreased velocity. For the small spacings ($H/D < 8$), the Nusselt number with the excitation St of 2.4 is lower than that of the non-excited jet due to the low turbulence intensity with the similar mean velocity in the potential core region for both excitation methods. As the gap distance increases, ($H/D > 8$) this trend is reversed and the high heat transfer rates are obtained with the excitation frequency of $St = 2.4$(m) and $St = 2.4$(s) because of the longer potential core length and the similar turbulence intensity for $H/D > 8$. For the case of $St = 1.2$(m) and $St = 1.2$(s), the Nusselt numbers are slightly higher than those of the non-excited jet at the small gap distance. At

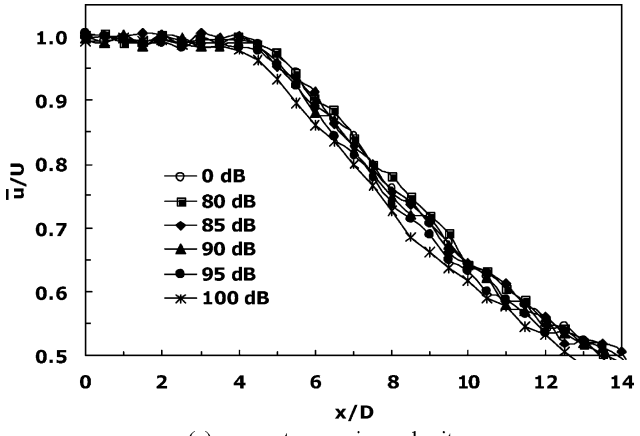

(a) mean streamwise velocity

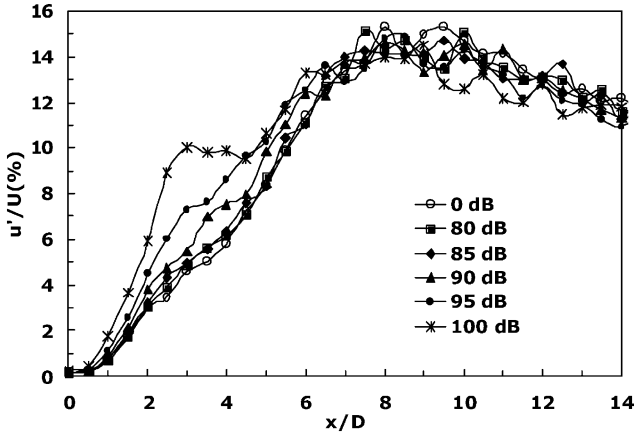

(b) turbulence intensity

Fig. 7. Effects of excitation level (dB) on velocity and turbulence distributions along the centerline for $St = 1.2$ with the shear layer excitation ($Re = 34{,}000$).

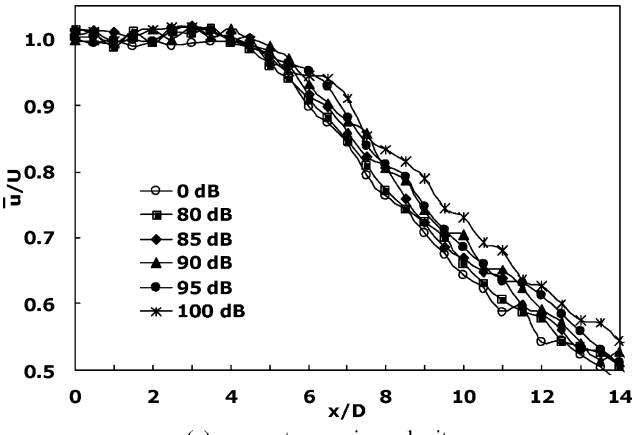

(a) mean streamwise velocity

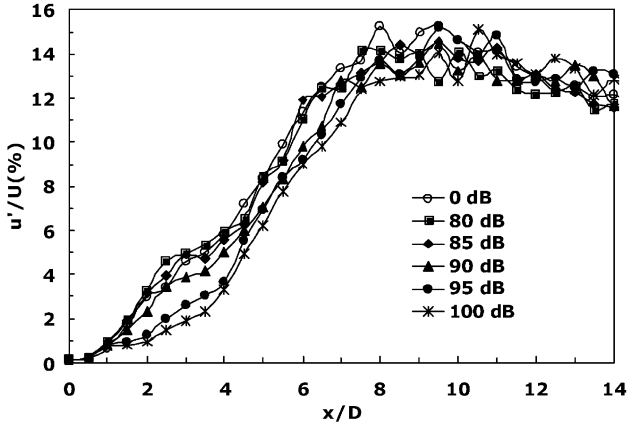

(b) turbulence intensity

Fig. 8. Effects of excitation level (dB) on velocity and turbulence distributions along the centerline for $St = 2.4$ with the shear layer excitation ($Re = 34{,}000$).

the large nozzle-to-plate distance of $H/D = 12$ and 16, the Nusselt number at the stagnation point are slightly lower than those of the non-excited jet because the jet velocity has a low value with the shorter potential core length. The entire trends of Nusselt number at the stagnation point are similar for the both excitation methods.

As explained above, excitation methods of the main jet excitation and the shear layer excitation are different in the flow scheme and the location of the actuator. However, effects on the flow and heat transfer of the jet flows with the acoustic excitation are similar in both methods.

3.3. Effects of excitation level (dB)

3.3.1. Flow characteristics

The flow and heat transfer characteristics of an impinging jet are affected not only by the excitation frequency (St) but also by the excitation level (dB).

Figs. 7 and 8 show the effects of excitation level on velocity and turbulence intensity for the shear layer excitation with the excitation frequency of $St = 1.2$ and 2.4, respectively. The excitation level varies from 80 to 100 dB at the nozzle exit. The excitation level of 0 dB indicates the non-excited jet. In case of $St = 1.2$ (Fig. 7), the flow has relatively lower velocity and high turbulence intensity than that of the non-excited jet as shown in Fig. 2 due to the promotion of the flow development and vortex pairing process. These tendencies are not clearly shown at the low excitation level ($\leqslant 90$ dB). However, the effects of the acoustic excitation appear clearly at the high excitation level (90 dB $\sim$). For the excitation St of 2.4, the effects on the flow by the acoustic excitation increase as the excitation power levels (dB) increase, as shown in Fig. 8. The velocity and turbulence distributions with increasing excitation level (dB) at $x/D = 0$, 4, 8 and 12 are shown in Fig. 9.

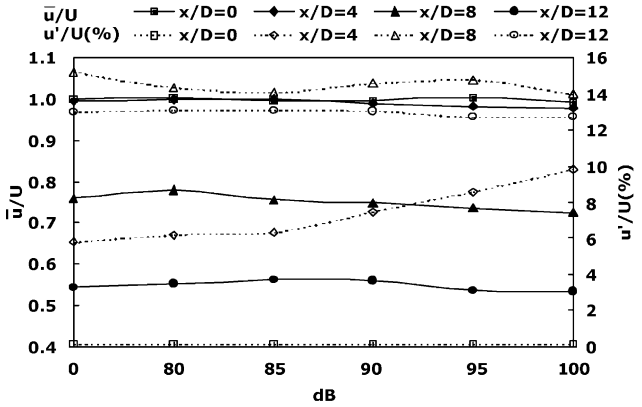

(a) St=1.2

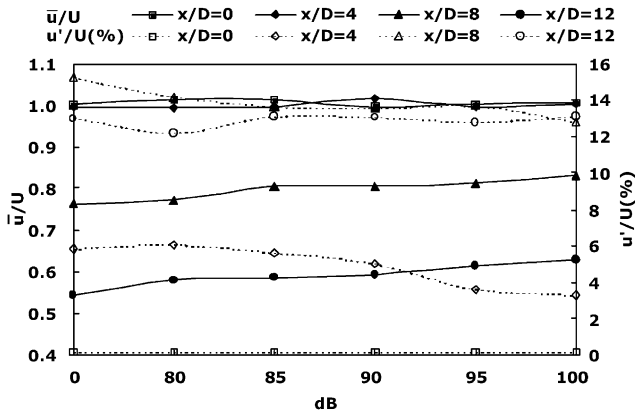

(b) St=2.4

Fig. 9. The mean streamwise velocity and turbulence distributions with increasing dB at $x/D = 0$, 4, 8 and 12 ($Re = 34{,}000$).

3.3.2. Heat transfer characteristics

Figs. 10 and 11 show the Nusselt number distributions with increasing excitation power levels for the excitation frequency of $St = 1.2$ and 2.4, respectively. In the case of $St = 1.2$ (Fig. 10), which promotes the flow

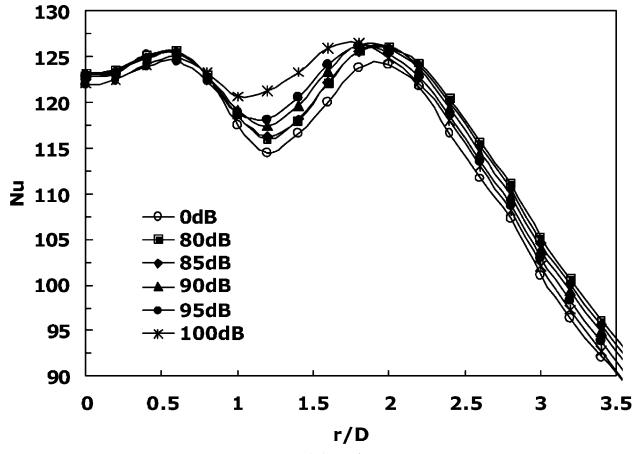

(a) H/D=2

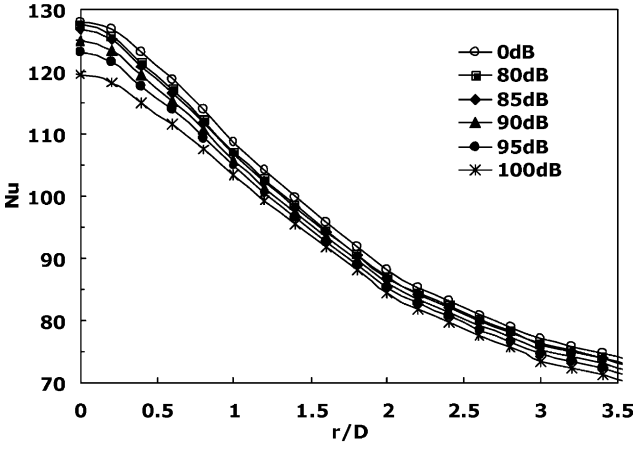

(b) H/D=12

Fig. 10. Nu distributions with increasing dB for $St = 1.2$ with the shear layer excitation ($Re = 34{,}000$).

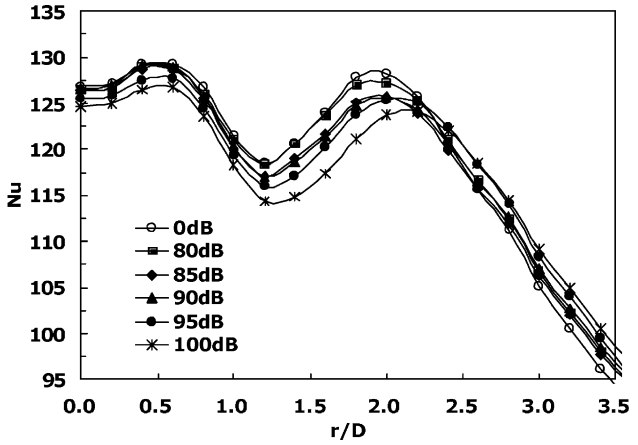

(a) H/D=2

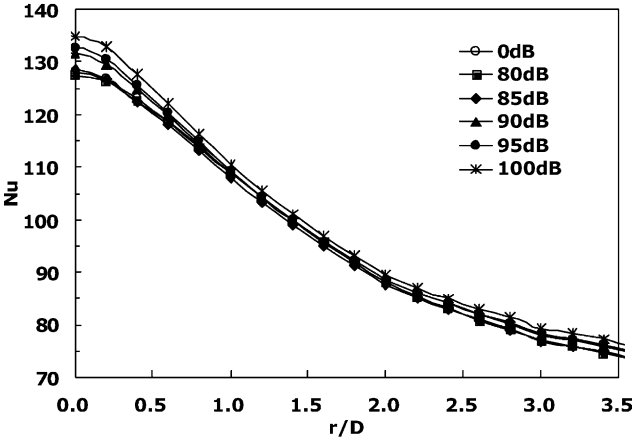

(b) H/D=12

Fig. 11. *Nu* distributions with increasing dB for $St = 2.4$ with the shear layer excitation ($Re = 34{,}000$).

development, the Nusselt number increases around $r/D = 1.3$ for the small gap distance of $H/D = 2$, as the excitation power levels increase. The reason is that the flow has the high turbulence intensity at the high excitation level resulting in promoting quickly the flow transition to the turbulence. With the excitation level of 100 dB, the position of the secondary peak in the Nusselt number even moves inward due to the significant promotion of the flow development. For the large gap distance of $H/D = 12$ (Fig. 10(b)), lower heat transfer rates are obtained as the excitation levels increase because the velocity at the jet center region decreases quickly with the fast jet flow development. For the excitation *St* of 2.4 (Fig. 11), which suppresses the flow development and vortex pairing process, the elevated power level delays the flow transition to the turbulent flow at the small gap distance of $H/D = 2$, resulting in movement of the secondary peak in the Nusselt number and lower heat transfer rates with lower turbulence intensity. These trends are reversed at large nozzle-to-plate distance ($H/D = 12$) because the jet flow has longer potential core with the higher power level.

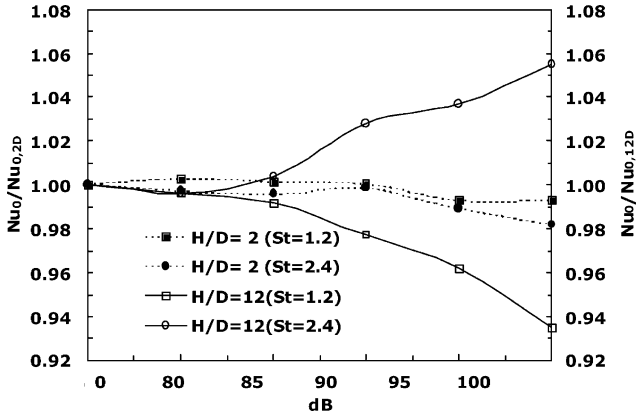

Fig. 12. Comparison of *Nu* at the stagnation point with increasing dB with the shear layer excitation ($Re = 34{,}000$).

Fig. 12 presents the comparison of the Nusselt number at the stagnation point with increasing the excitation level. For the excitation *St* of 1.2, the Nusselt number decreases as dB increases at $H/D = 12$. For the excitation *St* of 2.4, the Nusselt number increases with increasing dB at $H/D = 12$.

As a result, the flow and heat transfer characteristics of an impinging jet are affected by the excitation level. The effects of the acoustic excitation on the flow and heat transfer increase monotonously with increasing excitation power level at a given excitation frequency. Therefore, the excitation frequency and the excitation power level are both important factors in the acoustic excitation.

4. Conclusion

Flow structures of a jet are affected strongly by the nozzle exit conditions and the vortices generated around the jet periphery. Hence, the flow characteristics of an impinging jet can be changed largely by the control of vortex pairing and flow development. In this study, the effects of the acoustic excitation with the different excitation methods, based on the locations of the actuator, of the main jet excitation and the shear layer excitation on the heat/flow characteristics and the effects of the excitation level (dB) are investigated.

The similar flow and heat transfer characteristics are obtained with both excitation methods of the main jet excitation and the shear layer excitation though the basic flow schemes and the location of the forcing actuator are different. For the jet flow forced by the acoustic excitation of $St = 1.2$, the jet flow has a shorter potential core length and a slightly higher turbulence intensity than that of the not-excited jet. In the case of $St = 2.4$, the vortex pairing is suppressed

and the development of jet flow is delayed resulting in the longer potential core length with lower turbulence intensity. Heat transfer characteristics on the impingement surface are affected by the change of jet flow structures. As the development of jet flow is promoted by the acoustic excitation St of 1.2, the heat transfer rates are enhanced a little at the small gap distances with the high turbulence intensity. The heat transfer rates decreases slightly at the large gap distances due to the lower jet stream velocity. Conversely, for the acoustic excitation St of 2.4, the heat transfer rates are reduced a little at the short gap distances and the formation of the secondary peak of the heat transfer coefficients is delayed due to the low turbulence intensity of the jet core flow. Enhancements in the heat transfer are obtained at the large gap distances by the suppression of vortex pairing and the development of the jet resulting in the extended potential core length with $St = 2.4$.

The flow and heat transfer characteristics of an impinging jet with the acoustic excitation are also influenced by the excitation power level (dB). The effects of the acoustic excitation to the jet flow increase as excitation levels increase, and the effects of acoustic excitation may not appear clearly at the low excitation power level. Therefore, the excitation frequency and the excitation power level are both important factors in the acoustic excitation.

Acknowledgements

This work was supported by the National Research Laboratory program of KISTEP (Korea Institute of Science and Technology Evaluation and Planning).

References

Cho, H.H., Lee, C.H., Kim, Y.S., 1998. Characteristics of Heat Transfer in Impinging Jets by Control of Vortex Pairing. ASME paper No. 98-GT-276.

Crow, S.C., Champagne, F.H., 1971. Orderly structure in jet turbulence. J. Fluid Mech. 48 (3), 547–591.

Gardon, R., Akfirat, J.C., 1965. The role of turbulence in determining the heat transfer characteristics of impinging jets. Int. J. Heat Mass Transfer 8, 1261–1272.

Gau, C., Sheu, W.Y., Shen, C.H., 1997. Impingement cooling flow and heat transfer under acoustic excitations. J. Heat Transfer 119, 810–817.

Hoogendoorn, C.J., 1977. The effect of turbulence on heat transfer at a stagnation point. Int J. Heat Mass Transfer 20, 1333–1338.

Huang, L.M., El-Genk, M.S., 1994. Heat-transfer of an impinging jet on a flat surface. Int. J. Heat Mass Transfer 37, 1915–1923.

Hwang, S.D., Lee, C.H., Cho, H.H., 2001. Heat transfer and flow structures in axisymmetric impinging jet controlled by vortex pairing. Int. J. Heat Fluid Flow 22, 293–300.

Jambunathan, K., Lai, E., Moss, M.A., Button, B.L., 1992. A review of heat transfer data for single circular jet impingement. Int. J. Heat Fluid Flow 13, 106–115.

Kline, S.J., McClintock, F.A., 1953. Describing uncertainties in single sample experiments. Mechanical Engineering 75, 3–8.

Lee, C.H., Kim, Y.S., Cho, H.H., 1998. Heat transfer characteristics on impingement surface with control of axisymmetric Jet(1)—Uniform Velocity Distribution Jet—. Trans. KSME(B) 22, 386–398.

Liu, T., Sullivan, J.P., 1996. Heat transfer and flow structures in an excited circular impinging jet. Int. J. Heat Mass Transfer 39, 3695–3706.

Martin, H., 1977. Heat and mass transfer between impinging gas jets and solid surfaces. Adv. Heat Transfer 13, 1–60.

Morel, T., 1977. Design of two-dimensional wind tunnel contractions. J. Fluids Eng. 99, 371–378.

Viskanta, R., 1993. Heat transfer to impinging isothermal gas and flame jets. Expt. Thermal Fluid Sci. 6, 111–134.

Zaman, K.B.M., Hussain, A.K.M.F., 1980a. Vortex pairing in a circular jet under controlled excitation. Part 1. General jet response. J. Fluid Mech. 101, 449–491.

Zaman, K.B.M., Hussain, A.K.M.F., 1980b. Vortex pairing in a circular jet under controlled excitation. Part 2. Coherent structure dynamics. J. Fluid Mech. 101, 493–544.